Geomechanics and Engineering, *Vol. 11, No. 4 (2016) 553-570*
DOI: http://dx.doi.org/10.12989/gae.2016.11.4.553

The influence of tunnelling on the behaviour of pre-existing piled foundations in weathered soil

Cheol-Ju Lee [1a], Young-Jin Jeon [1b], Sung-Hee Kim [1c] and Inn-Joon Park [*2]

[1] *Department of Civil Engineering, Kangwon National University, Korea*
[2] *Department of Civil Engineering, Hanseo University, Korea*

(*Received March 15, 2016, Revised May 18, 2016, Accepted June 03, 2016*)

Abstract. A series of three-dimensional (3D) parametric finite element analyses have been performed to study the influence of the relative locations of pile tips with regards to the tunnel position on the behaviour of single piles and pile groups to adjacent tunnelling in weathered soil. When the pile tips are inside the influence zone, which considers the relative pile tip location with respect to the tunnel position, tunnelling-induced pile head settlements are larger than those computed from the Greenfield condition. However, when the pile tips are outside the influence zone, a reverse trend is obtained. When the pile tips are inside the influence zone, the tunnelling-induced tensile pile forces mobilised, but when the pile tips are outside the influence zone, compressive pile forces are induced because of tunnelling, depending on the shear stress transfer mechanism at the pile-soil interface. For piles connected to a cap, tensile and compressive forces are mobilised at the top of the centre and side piles, respectively. It has been shown that the increases in the tunnelling-induced pile head settlements have resulted in reductions of the apparent factor of safety up to approximately 43% when the pile tips are inside the influence zone, therefore severely affecting the serviceability of the piles. The pile behaviour, when considering the location of the pile tips with regards to the tunnel, has been analysed in great detail by taking the tunnelling-induced pile head settlements, axial pile forces, apparent factor of safety of the piles and shear transfer mechanism into account.

Keywords: numerical modelling and analysis; piled foundations; soil-structure interaction; shear transfer mechanism; weathered soil

1. Introduction

Recently, there have been various tunnelling activities in urban areas, where tunnel excavation might affect the behaviour of pre-existing adjacent piled foundations. Tunnelling below or adjacent to existing piles will influence the serviceability and, eventually, stability of the piled foundations because of tunnelling-induced ground movement, causing pile deformations and changes in the axial pile force distributions (Lee 2012). Williamson (2014) has analysed all the relevant studies conducted so far in great detail. There have been a number of studies concerning this problem based on theoretical methods and laboratory tests or geotechnical centrifuge tests (Jacobsz 2002),

*Corresponding author, Professor, E-mail: geotech@hanseo.ac.kr
[a] Professor
[b] Research Student
[c] Research Student

http://www.techno-press.org/?journal=gae&subpage=7 ISSN: 2005-307X (Print), 2092-6219 (Online)

Lee and Ng 2005, Ong *et al*. 2005, Pang 2006, Cheng *et al*. 2007, Lee and Chiang 2007, Marshall 2009, Lee 2012, 2013, Ng *et al*. 2013, Dias *et al*. 2014a, b, Hartono *et al*. 2014, Liu *et al*. 2014, Ng and Lu 2014, Ng *et al*. 2014 and Williamson 2014). Compared to these works, field measurements from full-scale tests are rather limited. Selemetas (2005), Pang (2006), Liu *et al*. (2014), Mair and Williamson (2014) and Williamson (2014) have reported observed pile behaviour from field measurements. Selemetas (2005) reported single pile response to nearby tunnelling based on full-scale tests in London clay. Pang (2006) also reported the behaviour of piles located laterally from the tunnel in a metro project in Singapore. Williamson (2014) reported the response of single piles and piled foundations to adjacent tunnelling from field measurements. Selemetas (2005) suggested a pile settlement prediction curve from the ground surface settlement profile and ground settlement at pile toe as a worst-case scenario. In addition, Devriendt and Williamson (2011) described two empirical methods (herein referred to as the assumed depth down pile method (*2/3 depth method*) and (*neutral axis method*) used in practice that can empirically estimate the tunnelling-induced pile head settlement using the Greenfield settlement profile and axial pile force distributions.

Attewell *et al*. (1986) proposed the tunnel influence zone based on field observations. Jacobsz (2002) reported the pile settlement influence zone from geotechnical centrifuge model tests on dry sand. In addition, Kaalberg *et al*. (2005) and Selemetas (2005) presented 3 different zones based on the ground surface settlements and pile settlements for undrained tunnelling in clay. Devriendt and Williamson (2011), Dias *et al*. (2014a, b), Hartono *et al*. (2014) and Marshall and Haji (2015) reported that the behaviour of piles was heavily dependent on the pile tip locations regarding the tunnel position. In addition, a tunnelling-induced tensile force or compressive forces have been observed depending on the pile tip locations. However, previous studies simply considered pile settlements when considering the tunnel influence zone for clay or dry sand, but the effect of the pile tip location with regards to the tunnel position on the pile response and, in particular, the shear stress transfer mechanism at the pile-soil interface remains rather poorly understood and unclear among engineers. Williamson (2014) reported tunnelling-induced settlements of up to approximately 40 mm of a building supported by a piled foundation with a cap, but the response of the piles connected to a cap has not been fully studied yet.

In this work, the behaviour of single piles and pile groups in response to tunnelling in weathered residual soil near the pre-existing piles and pile groups was studied by conducting a series of three-dimensional (3D) finite element analyses. In particular, the effect of the pile tip locations on the pile response has been fully studied. The effects of tunnelling on a single pile and on 5×5 pile groups with and without a cap were analysed by considering the tunnelling-induced pile head settlements, axial pile forces, the relative shear displacements, apparent pile capacity and the shear transfer mechanism at the pile-soil interface. In addition, the soundness of the above-mentioned empirical methods to estimate tunnelling-induced pile head settlements was examined, and the measured tunnelling-induced axial pile force distributions and deduced interface shear stresses reported by Selemetas (2005) and Williamson (2014) were also analysed with the computed results.

2. Numerical modelling

2.1 Finite element mesh and boundary conditions

In the current study, the three-dimensional (3D) finite element programme PLAXIS-3D (Brinkgreve *et al*. 2015) was used for the numerical analyses to study the effects of adjacent tunnelling on the behaviour of single piles and pile groups with and without a pile cap. The PLAXIS-3D programme is a special purpose three-dimensional finite element programme used to perform deformation and stability analysis for various types of geotechnical applications. The soil volume in PLAXIS-3D is modelled by 10-noded tetrahedral elements in the 3D mesh procedures (Brinkgreve *et al*. 2015). The piles and shotcrete are modelled as solid elements. Single piles and 5×5 pile groups with a centre-to-centre spacing of 2.5d were modelled to study the behaviour of the pile groups, where d is the pile diameter. Fig. 1 shows a representative 3D finite element mesh that was used in the numerical analyses for free-headed 5×5 piles. The tunnel diameter D in the analysis was 8 m, and the tunnel springline was located at a depth of 26 m below the ground surface, as shown in Figs. 2(a) and (b). The ground was assumed to be weathered residual soil. The piles were assumed to be 20 m in length L and 0.5 m in diameter d. The pile base was assumed to rest at an elevation of 2 m above the tunnel crown. In the analyses, different pile locations with respect to the tunnel position were considered to study the effects of the relative pile tip location on the pile behaviour. The locations of the single piles and the pile groups were arranged to be at offsets of 0D-3.0D, where D is the tunnel diameter. The distance between the tunnel centreline and the centre of the single piles and centre of pile groups in the traverse direction was specified as X_p for reference, as shown in Figs. 2(a) and (b). Based on the geometry, when X_p = 0D and 0.5D, the pile tips are inside the tunnel influence zone, and when X_p = 1D – 3D, pile tips are outside the tunnel influence zone. In the current study, the piles inside the groups were assumed to be either free-headed isolated piles or piles connected to a cap. The 0.5 m thick pile cap was located 0.5 m above the top of the soil, as shown in Fig. 2(b).The positions of the piles inside the pile groups referred to in the current study are shown in Fig. 2(c). The bottom of the mesh was pinned, and its lateral boundaries were supported by rollers. It was assumed that the tunnelling was conducted by using the new Austrian tunnelling Method (NATM). Table 1 summarises the numerical analyses conducted in the current study.

2.2 Constitutive models and material parameters

An elasto-plastic analysis was conducted to simulate tunnel construction and the pile-soil interaction trigger by tunnelling. The assumed material parameters summarised in Table 2 were taken from a previous study by Lee (2012) for weathered residual soils. An isotropic elastic model was used for the pile, the pile cap and shotcrete lining, and a Mohr-Coulomb model governed by non-associated flow rules with an isotropic elastic modulus was used for the residual soil. It was assumed that the material parameters of the pile and the cap were identical for simplicity. The pile-soil interactions at the pile-soil interface were included by using interface elements at the sides and bases of the piles to allow for soil slip when plastic soil yielding developed, as shown in Figs. 2(a) and (b). Interfaces are joint elements to allow for a proper modelling of the soil-structure

Table 1 Summary of numerical analyses

Analysis series	Single pile/pile group	Remarks
L	Single pile	Pile load test (no tunnelling)
Gr	-	Greenfield (no pile)
S	Single pile	Single pile
G	Pile group	5×5 group (free-headed)
C	Pile group	5×5 group (cap)

interaction and can be used to simulate the thin zone of intensely shearing material at the contact between a pile and the surrounding soil (Brinkgreve *et al*. 2015). An elasto-plastic model is used to describe the soil structure interaction behaviour at the pile-soil interface based on the Coulomb failure criterion. The reduction in the shear strength parameters at the pile-soil interface associated with the pile installation effect was considered using the following Eqs. (1) and (2)

$$c'_{inter} = R_{inter} \times c' \tag{1}$$

$$\phi'_{inter} = \tan^{-1}(R_{inter} \times \tan(\phi')) \tag{2}$$

Where c'_{inter} is the adhesion at the interface, R_{inter} is the strength reduction factor at the interface (0.7), c' is the cohesion of the residual soil, ϕ'_{inter} is the interface friction angle (26.1°) and ϕ' is the internal friction angle of the residual soil.

Table 2 Material parameters used in the numerical analyses

Material	Model	E (MPa)	c' (kPa)	ϕ' (°)	K_o	ν'	γ (kN/m^3)
Soil	Mohr-Coulomb	80	50	35	0.75	0.35	20
Pile/Cap	Elastic	30,000	-	-	-	0.20	25
Shotcrete lining		5,000 (s*) 15,000 (h*)	-	-	-	0.20	25

Notation: E (Young's modulus), c' (cohesion), ϕ' (internal friction angle), K_o (lateral earth pressure coefficient at rest), ν' (Poisson's ratio) and γ (unit weight of material)

* Note: *s* (soft shotcrete) and *h* (hard shotcrete)

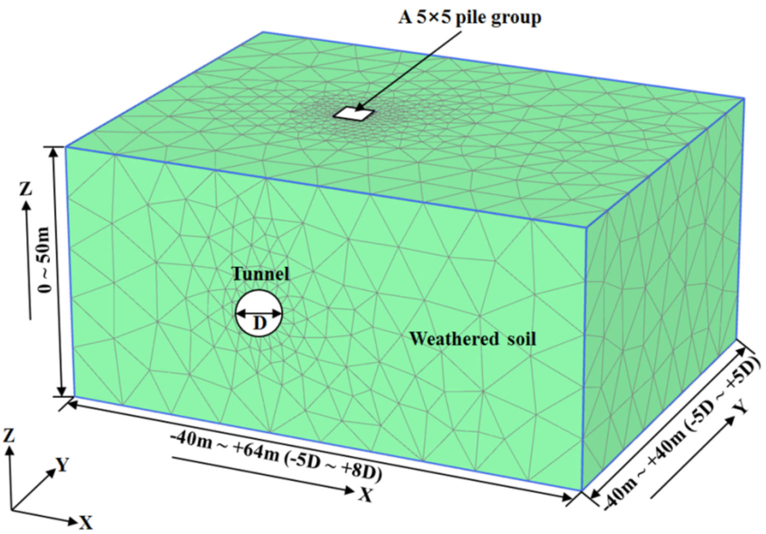

Fig. 1 Finite element mesh used in the current study (a 5×5 free-headed pile group, D: tunnel diameter)

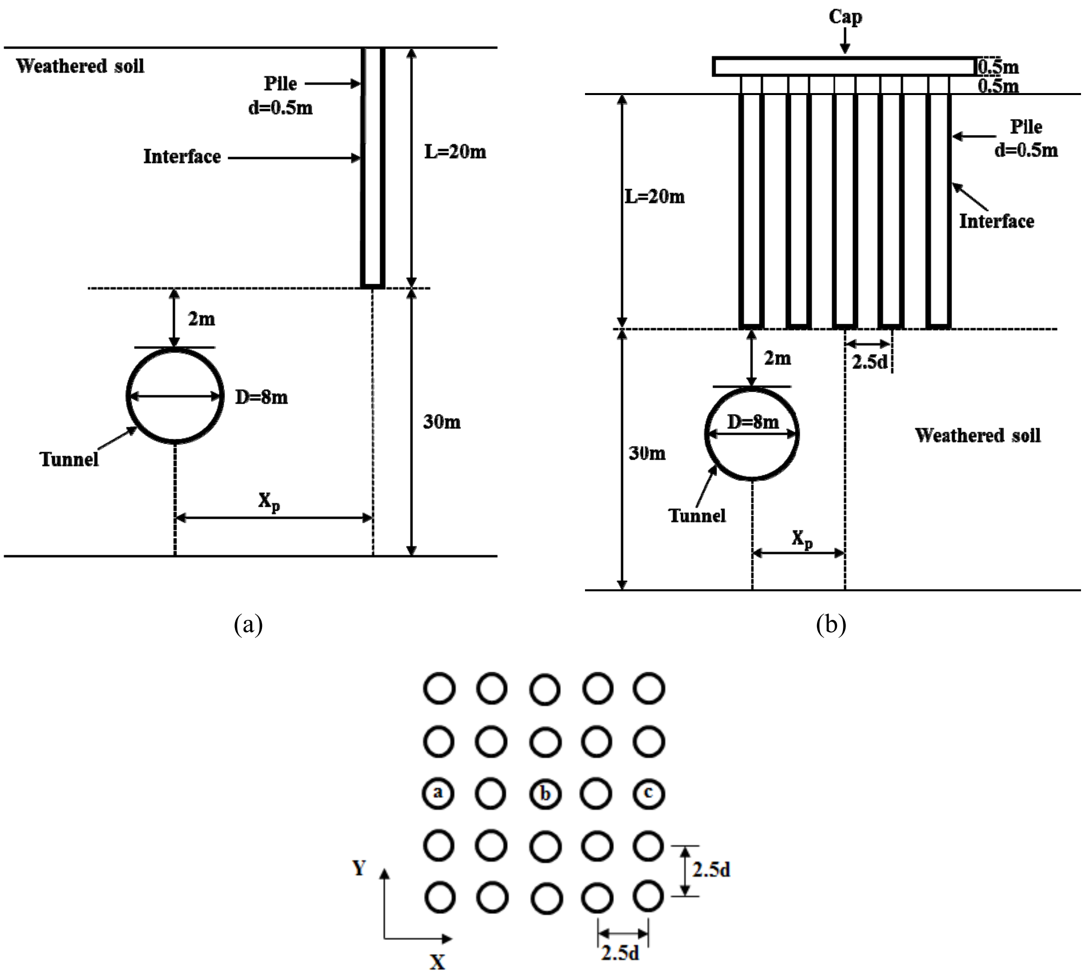

(a) (b)

(c)

Fig. 2 (a) Sectional view of analysis geometry (single pile) (not to scale); (b) Sectional view of analysis geometry (a 5×5 pile group connected to a cap) (not to scale); (c) Locations of piles inside a 5×5 group referred in the current study (a & c: side, b: centre)

2.3 Numerical modelling procedure

The numerical modelling consisted of three steps, initial geostatic equilibrium, application of an axial pile load simulating design pile load and staged tunnel construction. Tunnel excavation was simulated from –5D to +5D (–40 m to +40 m) in the longitudinal direction (Y), as shown in Fig. 1. The pile axis was located at X/D=0 and Y/D=0.0. Following the initial geostatic step, an axial load of 1,715 kN (determined from the simulation of the pile loading test, to be discussed in Section 3.1) was applied on the pile head to simulate the service loading prior to tunnel excavation. At each step, the tunnel was excavated in a 1 m increment. Hence, in any tunnel advancement, the unsupported tunnel length in the longitudinal direction was 1 m. After the excavation step, a shotcrete lining 200 mm thick was applied on the excavated soil face by specifying the material parameters corresponding to soft shotcrete (E = 5GPa), as explained by Lee (2012). Then, the elastic modulus of the soft shotcrete was changed to that of hard shotcrete (E = 15GPa) in the next excavation step. Upon completion of the numerical analysis, the axial pile force on the pile P was calculated as $P = \sigma_{zz)avg} \times A_p$, where $\sigma_{zz)avg}$ is the averaged vertical stress components in the pile elements at a certain elevation and A_p is the cross-sectional area of the pile. Similarly, the relative shear displacements and the interface shear stresses were also averaged.

3. Computed behaviour of the single piles and piles inside the pile groups

3.1 Determination of the allowable pile capacity (*Analysis L*)

A series of incremental axial pile loadings was applied on the pile head to simulate a pile loading test, which allows for the quantification of the load-settlement relation of the single pile. Analysis L was performed with boundary conditions identical to those in Fig. 2(a) and with the same material parameters, but the tunnel excavation was not included. Fig. 3 shows the relationship between the axial pile loading and pile head settlement computed from this analysis to decide the allowable pile capacity for the single pile. This curve may enable the study of tunnelling effects on the pile response regarding the change of the apparent pile capacity. A nearly linear relation was obtained between the axial pile force and the pile head settlement up to an axial pile loading of approximately 3,000 kN. However, after that threshold, a sudden increase in the pile settlement was observed with increased axial pile force, signifying the development of plastic yielding of the soil adjacent to the pile. In the current study, the widely used Davisson (1972) method was applied to determine the allowable pile capacity. The Davisson (1972) empirical envelope consists of an elastic compression line and an offset, as shown in Fig. 3. The computed load-settlement curve and the Davisson (1972) envelope match when the axial pile force is approximately 3,430 kN; hence, an ultimate pile capacity of 3,430 kN was obtained, as shown in Fig. 3. Then, using a factor of safety of 2.0, the allowable pile capacity P_a was obtained to be

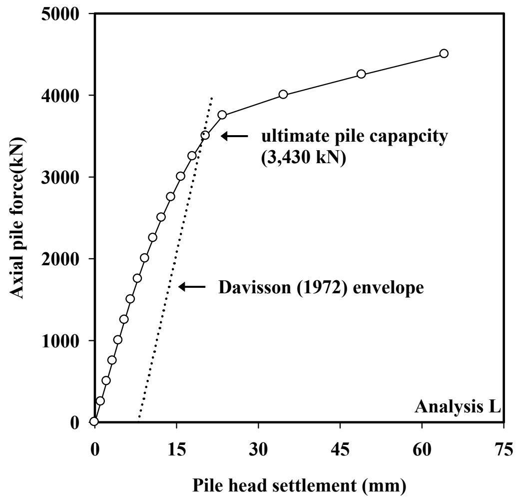

Fig. 3 Relation of axial pile force and pile head settlement

1,715 kN with a pile head settlement δ_i of 7.7 mm. Therefore, an axial pile force of 1,715 kN was applied on the pile head prior to tunnelling in the other analyses. For the free-headed pile groups, the allowable axial pile force was applied to each pile head individually, and for the piles connected to the cap, a uniform stress equivalent to the allowable axial pile force was applied on the top of the cap. The pile settlements in response to the service pile loading for the free-headed piles inside the pile group and the piles inside the cap were much larger than the single pile settlement and were approximately 3.5-3.9δ_i and 3.5δ_i, respectively, depending on the pile position inside the groups, as expected, because of the superposition of individual pile settlements (Fleming *et al*. 1992). It is noted that the settlements of the piles connected to the cap were almost the same as the settlements of the piles and were restrained because of the rigidity of the cap.

3.2 Settlement of the ground and piles (analyses Gr, S, G and C)

Settlements of the ground and piles

Figs. 4(a) and (b) show changes in the normalised tunnelling-induced pile head settlement $\delta_p/\delta_{gr)\max}$ and the soil surface settlement $\delta_g/\delta_{gr)\max}$ (Greenfield analysis) for all tunnel excavation steps (Y/D = –5 to +5) from the single pile and pile group analyses, where δ_p is the tunnelling-induced pile head settlements excluding pile settlement developed under application of the axial pile loading discussed in Section 3.1; $\delta_{gr)\max}$ is the maximum soil surface settlement at the centre pile location, computed from the Greenfield condition (5.9 mm); and δ_g is the soil surface settlement at the pile centre location, computed from the Greenfield condition. The pile settlements prior to tunnelling were zeroed, and hence, only tunnelling-induced pile settlements were considered. In the case of the free-headed piles inside the groups, the settlements at the centre and side piles are considered here. In the case of the piles connected to the cap, settlements only at the centre pile are considered because all pile settlements are nearly the same. The locations of the free-headed piles inside the pile groups and the piles connected to the cap referred in the current study are shown in Fig. 2(c).

Fig. 4(a) shows that the normalised pile head settlements computed from the single piles at different pile tip locations (X_p) gradually increase as the tunnel is excavated. The final normalised pile head settlements at different pile tip locations show that the longer the lateral distance from the tunnel centre is, the smaller the pile settlements are. When X_p = 0D and 0.5D, the values of $\delta_p/\delta_{gr)\max}$ are approximately 1.50 and 1.25, respectively, whereas when X_p = 1D and 2D, the values of $\delta_p/\delta_{gr)\max}$ are 0.93 and 0.5. Therefore, the magnitude of the pile head settlements with respect to the Greenfield settlement is dependent on the locations of the pile tips, and hence, it is anticipated that the shear transfer mechanism may also be different. This finding is similar to the previous research conducted by Dias and Bezuijen (2014a, b).

Fig. 4(b) shows that the $\delta_p/\delta_{gr)\max}$ values increased for the pile groups compared to the single pile settlement (X_p = 0D). The analysis showed that the piles inside the pile group developed a larger pile settlement than that for the single pile. The maximum tunnelling-induced pile head settlements of the piles inside the group are approximately 20-30% larger than that computed from the single pile analysis. At the end of the tunnel excavation, the values of $\delta_p/\delta_{gr)\max}$ computed from the single piles, the pile groups and the piles with the cap were 1.5, 1.9-2.1 and 1.9, respectively. This result is attributed to the larger reduction in the vertical soil stress related to the tunnel excavation in the case of the pile groups and the smaller bearing capacity of the soil underneath the pile base, as discussed by Lee *et al*. (2010). Furthermore, the piles at the centre (pile-b) settled

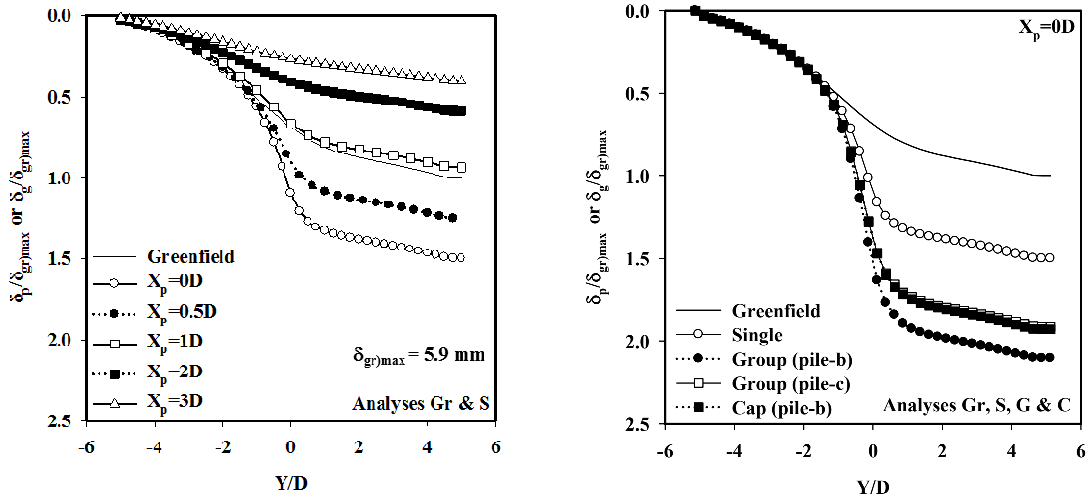

(a) (b)

Fig. 4 (a) Distributions of normalised tunnelling-induced pile head and soil surface settlements with tunnel advancement (single piles); (b) Distributions of normalised tunnelling-induced pile head and soil surface settlements with tunnel advancement (single piles and pile groups)

more than those at the corners (pile-c) in the pile groups.

The tunnelling-induced deformations and bending moments at the shotcrete lining near the tunnel crown for the single piles and the pile groups were nearly the same as those computed from the Greenfield condition. This result shows that no particular concern over the stability of the tunnel lining is required. In addition, the differential tunnelling-induced pile settlements inside the pile groups (free-headed and the cap) are negligible, and hence, it may not result in any concern on the stability of the piled foundations. Compared to the pile head settlements, the longitudinal and lateral pile deformation is insignificant, and hence, the tunnelling-induced bending moments on the piles are of small magnitude.

The tunnelling-induced pile head settlement estimated from the 2/3 depth method suggested by Devriendt and Williamson (2011) for the single pile was 8.4 mm, similar to the computed tunnelling-induced pile head settlement when X_p = 0D (8.9 mm). However, no tensile force was computed on the single piles in the current study, and hence, the neutral depth method (the distribution of the axial pile forces is discussed in Section 3.3) is applicable here. In addition, the deduced tunnelling-induced pile settlement for the single pile when X_p = 0D by using the pile settlement prediction curve proposed by Selemetas (2005) was 7.9-9.9 mm ($\delta_{gr)\max}$+ (2-4) mm), similar to the computed pile settlement. In addition, when the pile tips were at X_p = 1D and 2D, the computed pile head settlements were very close to the predictions [computed: X_p = 1D (5.5 mm), X_p = 2D (3.5 mm), predicted: X_p = 1D (5.1 mm), X_p = 2D (3.7 mm)]. This result shows that the settlement prediction curve can estimate tunnelling-induced pile head settlement for single piles with reasonable accuracy. However, because both methods are developed only for single piles, further effort may be required to estimate the pile settlements inside pile groups.

Settlement trough and tunnelling-induced pile settlement

Figs. 5(a) and (b) show the distribution of the normalised net soil settlement trough $\delta_g/\delta_{gr)\max}$

and the normalised tunnelling-induced pile settlement $\delta_p/\delta_{gr)\max}$ in the transverse direction (X direction in Fig. 1) upon completion of tunnel construction (Y/D = +5), computed from the analyses Gr, S, G and C. In the figures, the pile and soil settlements at the ground surface and the pile tip elevation are considered to study the relative displacements between the piles and the soil. Fig. 5(a) shows the pile head and soil surface settlements, and Fig. 5(b) shows pile and soil settlements at the pile tip location (Z/L = 1.0). When X_p = 0D and 1D, the tunnelling-induced pile settlements exceed the soil surface settlements, but as the lateral distance from the tunnel centre increases, the tunnelling-induced pile head settlements are smaller than the soil surface settlements (Fig. 5(a)). In particular, when X_p is larger than 1D, the tunnelling-induced pile settlements are slightly smaller than the soil settlement, and hence, it is expected that only little amount of shear strength may be mobilised. On the other hand, reverse distributions are observed at the pile tip location, as shown in Fig. 5(b), showing larger ground settlements at X_p = 0D and 0.5D and smaller settlement at X_p = 1D – 3D. The shear transfer mechanism will be discussed in later sections.

Distributions of the relative shear displacements

Figs. 6(a) and (b) show contour plots of the relative displacements between the single piles and the surrounding soil with depths at different values of X_p (0D and 2D). Here, the relative shear displacements ($\delta_{\text{pile}} - \delta_{\text{soil}}$) are the differences between the pile settlements, δ_{pile}, and the soil settlements, δ_{soil}, at a certain elevation [(+)ve: $\delta_{\text{pile}} > \delta_{\text{soil}}$, (–)ve: $\delta_{\text{pile}} < \delta_{\text{soil}}$]. When X_p = 0D, the pile settlements are larger than the soil settlements at the upper part of the pile, whereas near the pile tip, the ground settlements are larger than the pile settlement. However, when X_p = 2D, the opposite trend is observed. It is noted that the relative displacements between left and right side of the pile are different at a certain depth consistent with a previous study reported by Lee (2012).In addition, on average, the absolute magnitude of the relative displacements is larger when X_p = 0D,

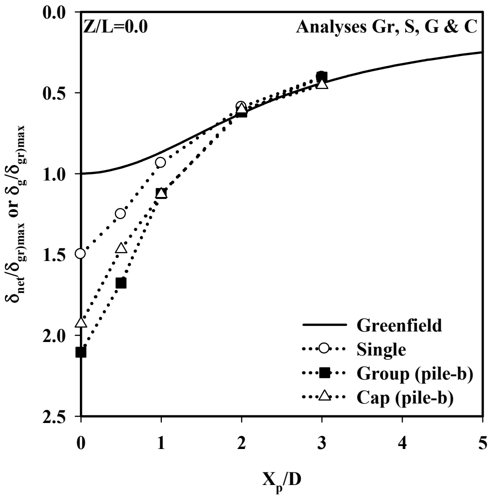

(a)

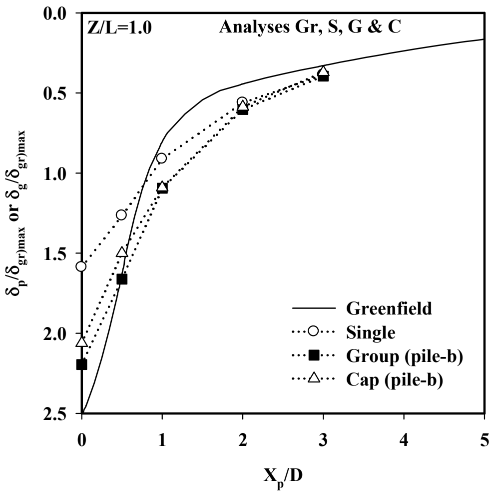

(b)

Fig. 5 (a) Distributions of normalised tunnelling-induced pile head and soil surface settlements in the lateral direction (single piles and pile groups); (b) Distributions of normalised tunnelling-induced pile and soil settlements at the pile tip location in the lateral direction (single piles and pile groups)

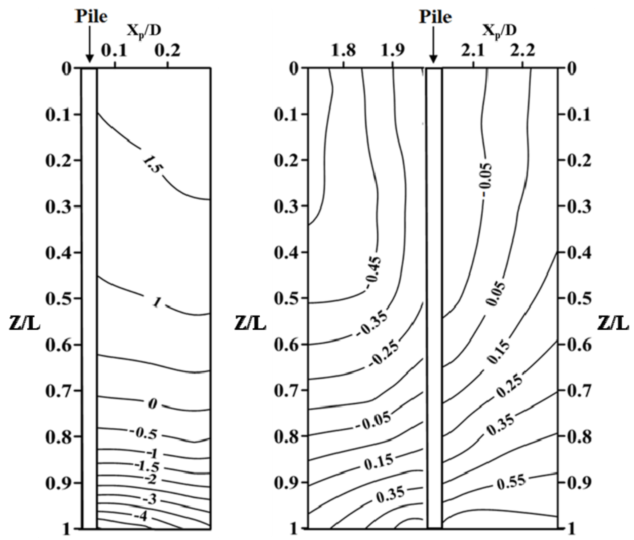

(a) (b)

Fig. 6 Distributions of relative shear displacements with depth (unit: mm)
(a: X_p = 0D, b: X_p = 2D) [(+)ve: $\delta_{\text{pile}} > \delta_{\text{soil}}$, (–)ve: $\delta_{\text{pile}} < \delta_{\text{soil}}$]

implying more shear transfer at X_p = 0D compared to when X_p = 2D. This result obviously demonstrates that the relative shear displacements and, hence, the shear transfer mechanism at the pile-soil interface may be different depending on the pile tip positions relative to the tunnel. Therefore, to study the tunnelling effect on the shear transfer mechanics at the pile-soil interface concerning the pile location needs to be rigorously researched. This will be discussed in the following sections in great detail.

3.3 Axial pile forces of single piles(*analysis S*)

Fig. 7(a) shows the distributions of the normalised axial pile force P/P_a computed from the single pile analysis (analysis S) with normalised pile depth (Z/L) at various pile locations upon the completion of tunnelling, where P is the axial pile force at a certain depth and P_a is the service pile loading prior to tunnelling. Prior to tunnel excavation, the axial pile forces decreased gradually with depth. Approximately 87% of the axial load was supported by the positive shaft resistance such that, at the pile tip, approximately 13% of the axial load was supported by the end bearing resistance. As X_p increased, the axial pile forces on the pile gradually decreased. A portion of the axial load carried by the pile base prior to tunnel excavation was now supported by the increased shear stresses associated with the change in the interface shear stress transfer mechanism, as discussed by Jacobsz (2002), Selemetas (2005), Devriendt and Williamson (2011), Hartono *et al.* (2014) and Mair and Williamson (2014). However, no tensile pile force was mobilised on the pile, and hence, there may not be any concern over the material integrity of the pile (Lee 2012).

Fig. 7(b) shows the tunnelling-induced normalised axial pile forces (P_{net}/P_a) for various pile tip locations with normalised pile depth (Z/L), where P_{net} is the tunnelling-induced axial pile force at a certain depth. The tensile forces are mobilised when X_p = 0D and 0.5D and maximum P_{net}/P_a values of 0.174 and 0.077 are computed for the piles at X_p = 0D and 0.5D, respectively. However,

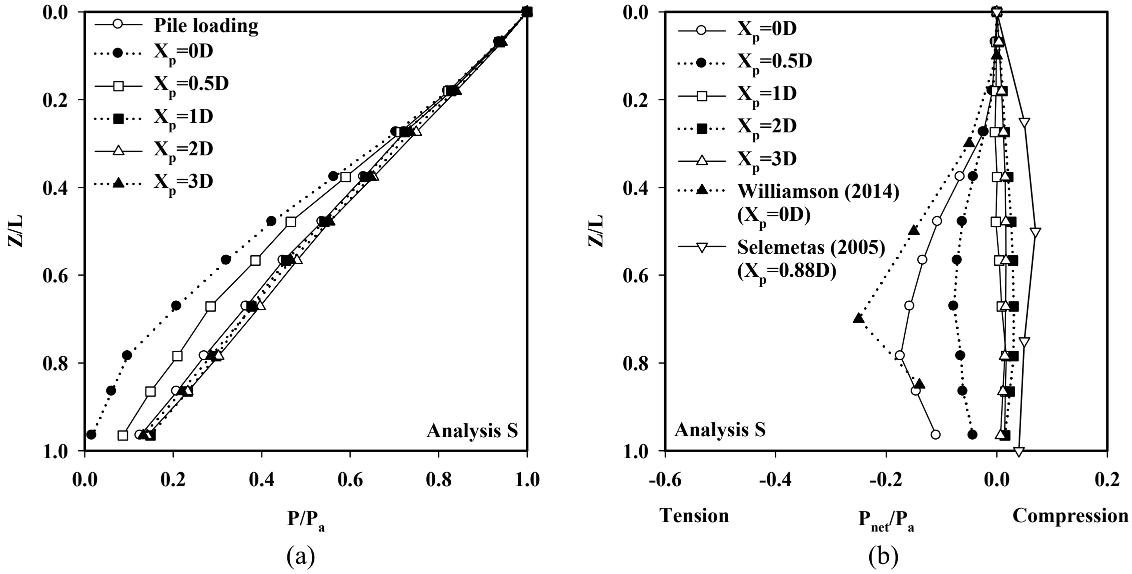

Fig. 7 (a) Distributions of normalised axial pile forces with depth (single piles); (b) Distributions of normalised tunnelling-induced axial pile forces with depth (single piles)

when the pile tip is X_p = 1D and 2D, the compressive tunnelling-induced pile forces are computed (P_{net}/P_a = 0.017 and 0.031). This result indicates that the skin friction at the pile-soil interface changes depending on the relative location of the pile tips. This is related to above-mentioned ground settlements, which are larger than the pile settlements mobilising downward shear stresses, similar to negative skin friction on piles (Lee 2012). Fig. 7(b) also shows the normalised tunnelling-induced axial pile force distributions deduced from the above-mentioned field measurements reported by Selemetas (2005) and Williamson (2014). This distribution is in general agreement with the computed results, but the magnitude of the measured tunnelling-induced pile forces is slightly different from the computed values, perhaps because large ground volume losses occurred at the site.

3.4 Axial pile forces of the pile group piles (analyses S, G and C)

Fig. 8 shows the distributions of tunnelling-induced axial pile forces for the single piles, free-head pile groups and piles connected to the cap at X_p = 0D. As reported by previous studies, smaller axial pile forces developed on the free-head piles inside the group compared to for the single pile (Lee 2012). In particular, a somewhat odd distribution is observed for piles with the cap near the pile head. Tunnelling induced tensile and compressive forces of 0.076 P_{net}/P_a and 0.035 P_{net}/P_a at pile-b and pile-c, respectively, above the soil surface, as demonstrated by a triangle and a circle in the figure. However, because their magnitudes are relatively small, the structural stability of the piles and the cap regarding the pull-out of the centre piles and/or punching failure of the cap may not be of concern. Because of the developments of the tension and compression near the pile head, the maximum and minimum P_{net}/P_a values developed on the centre and side piles connected to the cap, not on the single pile. The computed results show that the side pile settled slightly less than the centre pile because the shear stresses on the centre piles was larger than on the side piles.

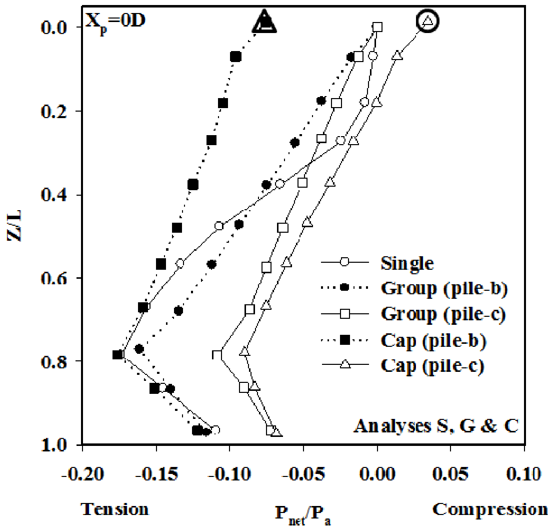

Fig. 8 Distributions of tunnelling-induced axial pile forces with depth (single piles & pile groups)

Thus, the centre piles tended to drag the cap down, whereas the side piles resisted the movement because the pile cap resulted in nearly uniform pile settlements. The interaction between the side piles, the centre piles, and the cap resulted in the development of tensile forces at the centre piles and compressive forces at the side piles through the redistribution of the axial forces among the piles. This is exactly opposite of the behaviour of piles connected to a cap subjected to down drag forces in consolidating ground (Lee *et al*. 2006).

3.5 Relative shear displacements at the interface (*analysis S*)

Fig. 9 shows the distributions of the tunnelling-induced relative shear displacements ($\delta_{\text{pile}} - \delta_{\text{soil}}$) at various pile tip locations for single piles. The relative movement mobilised prior to tunnelling is zeroed to quantify the net relative displacements, reflecting only the relative displacements triggered by tunnelling. When the pile tips are inside the tunnel influence zone (X_p = 0 – 0.5D) the relative displacements change with depth, whereas those when X_p = 1D – 3D are almost unchanged. When the pile tips are inside the tunnel influence zone (X_p = 0 – 0.5D), the pile settlements are larger than the soil settlements from the pile head to about Z/L = 0.7 – 0.75. Below Z/L = 0.7 – 0.75, however, the direction of the relative displacements reverse from positive to negative, implying that the soil settlements are now greater than the pile settlements. This result indicates the development of downward negative skin friction near the pile tip. Therefore, it can be concluded that the lower part of the soil adjacent to the pile tip drags the pile down because of soil settlement resulting from tunnel excavation, whereas the upper part of the soil resists the pile settlement in a reverse direction. However, on the other hand, opposite trends are observed when X_p = 1D – 3D. Therefore, the upper part of the soil adjacent to the pile drags the pile down, associated with tunnel excavation, whereas the lower part of the soil resists pile settlement in an opposite direction, resulting in compressive pile forces, as discussed previously. However, because the magnitude of the relative shear displacements in this case are insufficient for the full mobilisation of the interface shear strength, the tunnelling-induced compressive pile forces outside

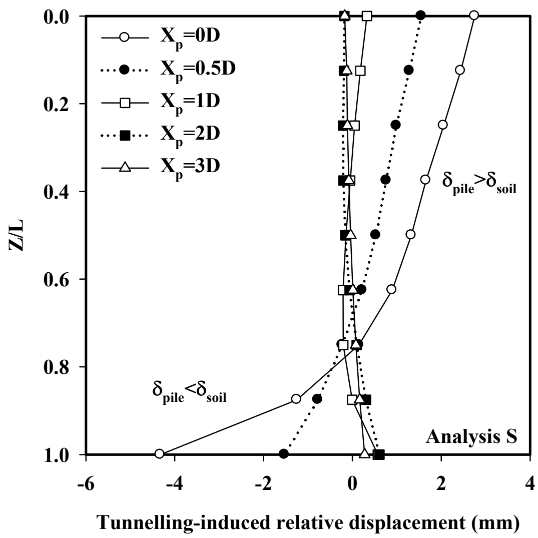

Fig. 9 Distributions of tunnelling-induced relative shear displacements with depth (single piles)

the tunnel influence zone are smaller than the tunnelling-induced tensile pile forces for piles inside the tunnel influence zone.

3.6 Interface shear stress at the interface (analysis S)

Fig. 10 shows the distributions of the tunnelling-induced shear stresses at various pile tip locations of the single piles, excluding the effect of axial pile loading prior to tunnelling. Major

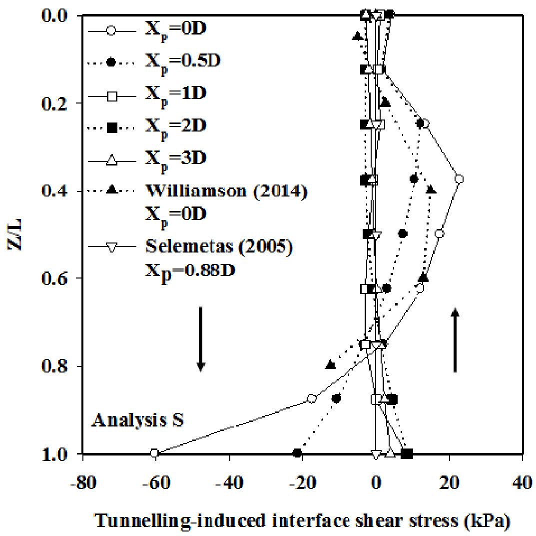

Fig. 10 Distributions of tunnelling-induced shear stresses with depth (single piles)

changes in the shear stresses develop when X_p = 0D and 0.5D. However, when X_p = 1 – 3D, the anges are of much smaller magnitudes. The arrows in the figure show the direction of the unnelling-induced interface shear stresses. Downward shear stresses are mobilised near the pile tip, triggering the pile head settlements, whereas upward resisting shear stresses are observed at the upper part of the piles when the pile tips are inside the tunnel influence zone (X_p = 0D and 0.5D). However, the opposite pattern is computed when X_p = 1D – 3D. This result is similar to the development of downward shear stresses at the upper part of the piles and the upward shear stresses near the pile tip subjected to negative skin friction (Lee *et al*. 2006). This trend is related to the above-mentioned distributions of the interface relative shear displacements at the pile-soil interface depending on the pile tip locations. Fig. 10 also shows the normalised tunnelling-induced interface shear stress distribution deduced from the above-mentioned axial pile force distribution by Selemetas (2005) and Williamson (2014). It is noted that the computed shear stress distribution deviates slightly from the measurements, but the trend of the distributions of the shear stresses is qualitatively similar.

3.7 Effect of the relative locations of the pile tips (*analyses Gr*, *S*, *G and C*)

Pile head settlements

Fig. 11(a) shows the distributions of the normalised Greenfield settlement $\delta_g/\delta_{gr)\max}$ at the ground surface and tunnelling-induced pile head settlements $\delta_p/\delta_{gr)\max}$ for the single piles, piles inside the groups and the piles connected to the cap upon completion of tunnelling at different values of X_p. In the case of the piles connected to the cap, only the pile settlements at the centre pile (pile-b) were considered because the pile settlements were almost constant regardless of the locations of the piles. It is noted that the maximum pile settlements developed when X_p = 0D and

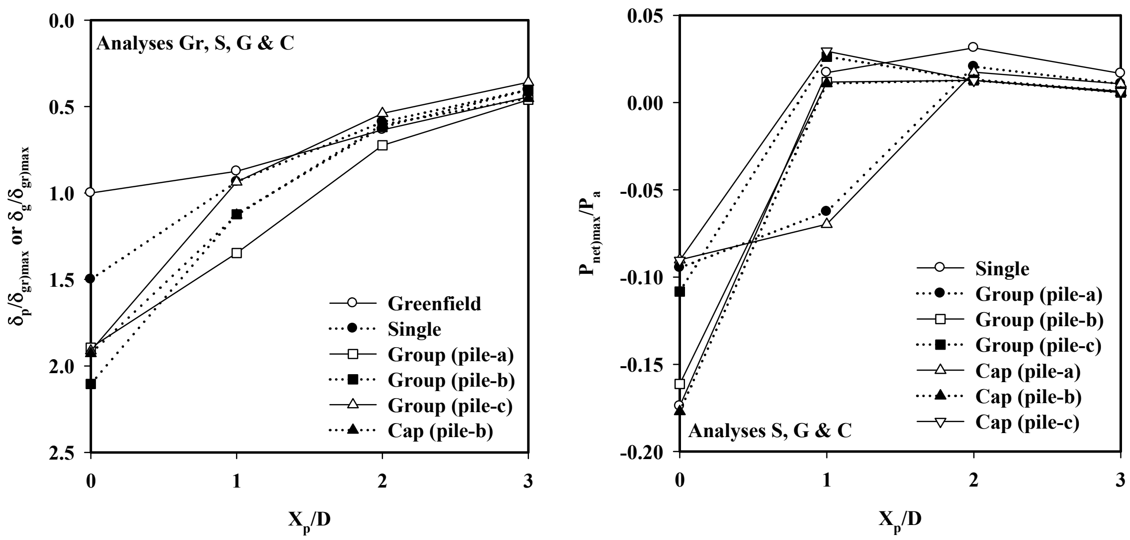

(a) (b)

Fig. 11 (a) Distributions of normalised pile head and soil surface settlements at different pile tip locations (single piles & pile groups); (b) Distributions of maximum tunnelling-induced axial pile forces at different pile tip locations (single piles & pile groups)

Table 3 Changes of the apparent factor of safety (FS) for the single piles

X_p/D	0	0.5	1	2	3
FS	1.10	1.18	1.29	1.47	1.59
δ_p (mm)	8.9	7.4	5.5	3.5	2.4

decreased with an increase in the lateral distances of the piles from the tunnel. As the lateral istance increased, the difference between the pile settlements gradually decreased. In addition, the iles inside the groups settled more than those in the single piles. When the pile tips are at X_p = 0D and 1D, the Greenfield settlements are smaller, whereas when the piles are outside the influence zone (X_p = 2D and 3D), the pile settlements are smaller, except for pile-a inside the group. The settlements of the piles connected to the cap are somewhat similar to the corresponding settlements at the centre pile of the free-headed pile groups. This result indicates that pile settlement is governed both by the lateral distance of the pile tips from the tunnel and the relative locations of the piles inside the pile group.

Maximum pile forces

Fig. 11(b) shows the normalised maximum tunnelling-induced pile forces $P_{\mathrm{net)max}}/P_a$ for the single piles, the piles inside the groups and the piles connected to the cap upon completion of tunnelling (analyses S, G and C) at different values of X_p. When the piles are inside the influence zone, tensile forces are mobilised, whereas compressive forces are computed for piles outside the influence zone. The maximum tensile force is mobilised at the centre pile connected to the cap at X_p = 0D because of the development of tensile forces near the pile head, as discussed previously. When the lateral distance from the tunnel increases, the absolute magnitudes of the maximum pile forces and the differences between piles decrease. Because their magnitudes are relatively small, these tunnelling-induced pile forces are unlikely to cause any structural integrity of the piles and the foundation system.

Apparent factor of safety

Table 3 shows the changes of the apparent factor of safety (FS) of the single piles with the tunnelling-induced pile head settlements δ_p. When the pile tip is directly above the tunnel crown (X_p = 0D), the final pile head settlement upon the completion of tunnelling is 16.6 mm [settlement due to axial pile load (7.7 mm) and tunnelling-induced settlement (8.9 mm) combined]. The apparent pile loading corresponding to the settlement of 16.6 mm in Fig. 3 is approximately 3,110 kN. Hence, the apparent pile capacity is reduced from 2.0 to 1.10 following Lee and Ng (2005) and Lee (2013) [FS = 3,430/3,110 (ultimate pile load/apparent pile load) = 1.10]. Similarly, the apparent FS of the piles are increased as the lateral distance from the tunnel centre is increased. It is worthwhile to note that, although the pile tip is outside the influence zone (X_p = 1D – 3D), the reduction of FS can be still significant. Overall, the average reductions in FS when the piles are inside and outside the tunnelling influence zone are 43% and 28%, respectively. This result shows that tunnelling-induced pile settlement can result in serious concerns over the serviceability of piled foundations, as reported by Lee and Ng (2005) and Selemetas (2005). Furthermore, it is likely that larger reductions in the apparent pile capacity are anticipated for the piles in the groups because of larger increases in the tunnelling-induced pile head settlements.

4. Conclusions

Three-dimensional numerical analyses have been conducted to study the behaviour of piled foundations affected by adjacent tunnel construction in residual soils. The effect of the relative locations of the pile tips with respect to the tunnel on the response of single piles and pile groups to tunnelling have been discussed in detail. The following conclusions can be drawn from the present study.

- It has been shown that the locations of the pile tips with regards to the tunnel position affect the pile response to tunnelling substantially. When the pile tips are inside the tunnel influence zone (X_p = 0D and 0.5D), tensile forces are mobilised on the single piles, whereas when the pile tips are outside the influence zone, compressive forces develop. However, compressive tunnelling-induced pile forces are computed for piles outside the tunnel influence zone. Tunnelling-induced forces on the piles are dependent on the distributions of the tunnelling-induced relative shear displacements at the pile-soil interface, governed by the relative locations of the pile tips with regards to the tunnel position, as is the shear stress transfer mechanism. The computed results show that the longer the lateral distance from the tunnel is, the smaller the tunnelling-induced pile forces and pile head settlements are. The empirical methods may make reasonable predictions on the tunnelling-induced pile head settlements for single piles.
- Smaller tunnelling-induced pile forces and larger pile head settlements are computed for the piles inside pile groups. Because of the smaller relative shear displacements at the interface, shear strength is only partially mobilised for piles inside groups compared to the single piles having larger degree of shear strength mobilisation. When the piles are connected to a cap, tensile forces and compressive forces are induced near the pile head at the inner and outer piles, respectively. However, their magnitudes are small and may not result in any concern over the stability of the foundation system.
- It has been shown that the serviceability of piles can be reduced substantially, especially for the pile groups, by considering tunnelling-induced pile settlements and the apparent factor of safety of the piles. When the pile tips were inside the tunnelling influence zone, the apparent factor safety decreased by up to approximately 43%. In addition, even though the tips were outside the tunnelling influence zone (X_p = 1D – 3D), the computed apparent factor of safety was reduced by approximately 28% on average. This result implies the possibility that tunnelling will affect the serviceability of piled foundations even though the pile tip is outside the influence zone. A further study concerning this issue needs to be conducted.

Acknowledgments

This study is supported by Kangwon National University. This research was supported by the Korea Agency for Infrastructure Technology Advancement under the Ministry of Land, Infrastructure and Transport of the Korean government. (Project Number: 13CCTI-T01).

References

Attewell, P.B., Yeates, J. and Selby, A.R. (1986), *Soil Movements Induced by Tunnelling and Their Effects on Pipelines and Structures*, Blackie and Son Ltd.

Brinkgreve, R.B.J., Kumarswamy, S. and Swolfs, W.M. (2015), *Plaxis 3D 2015User's Manual*, (Edited by R.B.J. Brinkgreve, S. Kumarswamy and W.M. Swolfs).

Cheng, C.Y., Dasari, G.R., Chow, Y.K. and Leung, C.F. (2007), "Finite element analysis of tunnel-soil-pile interaction using displacement controlled model", *Tunn. Undergr. Space Technol.*, **22**(4), 450-466.

Davisson, M.T. (1972), "High capacity piles", *Proceedings of Lecture Series in Innovations in Foundation Construction*, ASCE, Illinois Section, pp. 81-112.

Devriendt, M. and Williamson, M. (2011), "Validation of methods for assessing tunnelling-induced settlements on piles", *Ground Eng.*, 25-30.

Dias, T.G.S. and Bezuijen, A. (2014a), "Pile tunnel interaction: Literature review and data analysis", *ITA World Tunnel Congress 2014*, Iguassu Falls, Brazil, May, pp. 1-10

Dias, T.G.S. and Bezuijen, A. (2014b), "Pile-tunnel interaction: A conceptual analysis", *Proceedings of the 8th International Symposium on Geotechnical Aspects of Underground Construction in Soft Ground*, CRC Press, Seoul, Korea, August, **Volume 1**, pp. 251-255.

Fleming, W.G.K., Weltman, A.J., Randolph, W.F. and Elson, W.K. (1992), *Piling Engineering*, (2nd Edition), Blackie Academic & Professional.

Hartono, E., Leung, C.F., Shen, R.F., Chow, Y.K., Ng, Y.S., Tan, H.T. and Hua, C.J. (2014), "Behaviour of pile above tunnel in clay", *Phys. Model. Geotech.*, 833-838.

Jacobsz, S.W. (2002), "The effects of tunnelling on piled foundations", Ph.D. Thesis; University of Cambridge, UK.

Kaalberg, F.J., Teunissen, E.A.H., van Tol, A.F. and Bosch, J.W. (2005), "Dutch research on the impact of shield tunneling on pile foundations", *Proceedings of the 5th International Conference of TC 28 of the ISSMGE*, *Geotechnical Aspects of Underground Construction in Soft Ground*, London, UK, June, pp. 123-133.

Lee, C.J. (2012), "Three-dimensional numerical analyses of the response of a single pile and pile groups to tunnelling in weak weathered rock", *Tunn. Undergr. Space Technol.*, **32**, 132-142.

Lee, C.J. (2013), "Numerical modelling of pile response to tunnelling in stiff clay", *Comput. Geotech.*, **51**, 116-127.

Lee, C.J. and Chiang, K.H. (2007), "Responses of single piles to tunneling-induced soil movements in sandy ground", *Can. Geotech. J.*, **44**(10), 1224-1241.

Lee, G.T.K. and Ng, C.W.W. (2005), "The effects of advancing open face tunneling on an existing loaded pile", *J. Geotech. Geoenviron. Eng., ASCE*, **131**(2), 193-201.

Lee, C.J, Lee, J.H. and Jeong, S.S. (2006), "The influence of negative skin friction on piles in groups connected to a cap", *Geotechnique*, **56**(1), 53-56.

Lee, S.W., Choy, C.K.M., Cheang, W.W.L., Swolfs, W. and Brinkgreve. R. (2010), "Modelling of tunnelling beneath a building supported by friction bored piles", *Proceedings of the 17th Southeast Asian Geotechnical Conference*, Taipei, Taiwan, January, pp. 215-218.

Liu, C., Zhang, Z. and Regueiro, R.A. (2014), "Pile and pile group response to tunnelling using a large diameter slurry shield – Case study in Shanghai", *Comput. Geotech.*, **59**, 21-43.

Mair, R.J. and Williamson, M.G. (2014), "The influence of tunnelling and deep excavation on piled foundations", *Geotech. Aspect. Undergr. Construct. Soft Ground*, 21-30.

Marshall, A.M. (2009), "Tunnelling in sand and its effect on pipelines and piles", Ph.D. Thesis; University of Cambridge, UK.

Marshall, A.M. and Haji, T. (2015), "An analytical study of tunnel-pile interaction", *Tunn. Undergr. Space Technol.*, **45**, 43-51.

Ng, C.W.W. and Lu, H. (2014), "Effects of the construction sequence of twin tunnels at different depths on an existing pile", *Can. Geotech. J.*, **51**(2), 173-183.

Ng, C.W.W., Lu, H. and Peng, S.Y. (2013), "Three-dimensional centrifuge modelling of twin tunnelling effects on an existing pile", *Tunn. Undergr. Space Technol.*, **35**, 189-199.

Ng, C.W.W., Soomro, M.A. and Hong, Y. (2014), "Three-dimensional centrifuge modelling of pile group responses to side-by-side twin tunnelling", *Tunn. Undergr. Space Technol.*, **43**, 350-361.

Ong, O.W., Leung, C.F., Yong, K.Y. and Chow, Y.K. (2006), "Pile responses due to tunneling in clay",

Proceedings of the 6th International Conference on Physical Modelling in Geotechnics Physical Modelling in Geotechnics, London, UK, June, pp. 1177-1182.
Pang, C.H. (2006), "The effects of tunnel construction on nearby pile foundation", Ph.D. Thesis; The National University of Singapore, Singapore.
Selemetas, D. (2005), "The response of full-scale piles and piled structures to tunnelling", Ph.D. Thesis; University of Cambridge, UK.
Williamson, M.G. (2014), "Tunnelling effects on bored piles in clay", Ph.D. Thesis; University of Cambridge, UK.

GC